

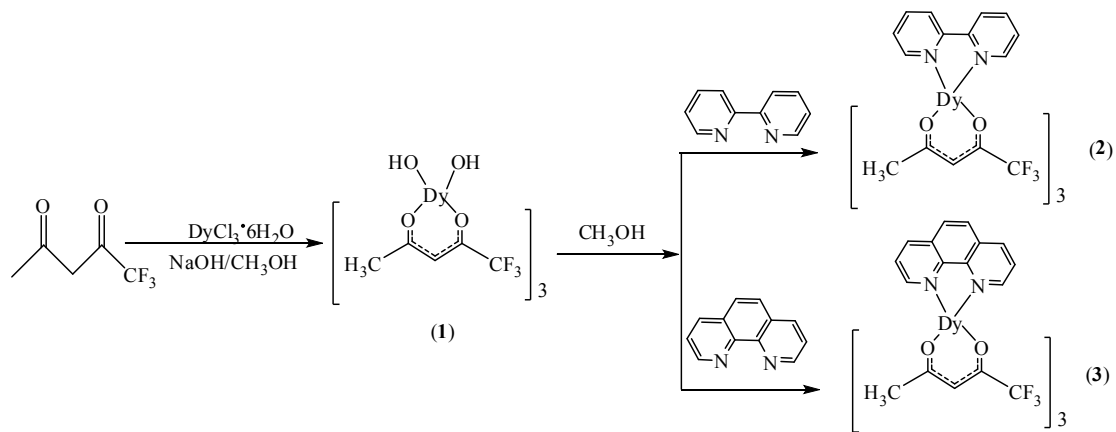
Electronic Supplementary Information

# Luminescent single molecule magnets of a series of $\beta$ -diketone dysprosium complexes

Wenyi Chu, Qingyan Sun, Xu Yao, Pengfei Yan, GuanghuiAn, Guangming Li\*

Key Laboratory of Functional Inorganic Material Chemistry (MOE), School of Chemistry and Materials Science, Heilongjiang University, No. 74, Xuefu Road, Nangang District, Harbin, Heilongjiang 150080, P. R. China, E-mail: gml\_i\_2000@163.com. Fax: (+86)451-86608458; Tel: (+86) 451-86608458

Scheme S1	Synthesis of complexes <b>1–3</b> .
Fig. S1	IR spectra of tfa and complexes <b>1–3</b> .
Fig. S2	UV-vis absorption spectra of tfa and complexes <b>1–3</b> in CH <sub>3</sub> OH (10 <sup>-5</sup> mol/L)
Fig. S3–5	TG–DSC curves of complexes <b>1–3</b> .
Fig. S6–8	The powder X-ray diffraction spectra of the simulated patterns and experimental for complexes <b>1–3</b> .
Fig. S9–11	The inter molecule $\pi$ – $\pi$ stacking and hydrogen bonds interactions in complexes <b>1–3</b> .
Fig. S12	M versus H / T plots at 1.8–8K for complexes <b>1–3</b> .
Fig. S13	Temperature dependence of the in-phase ( $\chi'$ ) and out-of-phase ( $\chi''$ ) ac susceptibility of complexes <b>1</b> (left), <b>2</b> (middle) and <b>3</b> (right), respectively, under zero dc field.
Fig. S14	Temperature dependence of the in-phase ( $\chi'$ ) and out-of-phase ( $\chi''$ ) acsusceptibility of complexes <b>1</b> (left), <b>2</b> (middle) and <b>3</b> (right) under 2000 Oe in the frequency range 10–1000 Hz in the temperature range of 2–18 K.
Fig. S15	Field dependence of the characteristic frequency as a function of the applied dc field for complexes <b>1</b> (a), <b>2</b> (b) and <b>3</b> (c) at 6 K.
Fig. S16	Fitted broadness parameters $\alpha_{\text{Cole}}$ as functions of temperature for complexes <b>1–3</b> .
Fig. S17	Hysteresis loops for complexes <b>1</b> (left) and <b>2</b> (right) with different sweep rate at 1.8K.
Fig. S18	Emission spectra of complexes <b>1–3</b> in the MeOH at 298 K (10 <sup>-5</sup> mol/L, $\lambda_{\text{ex}} = 335$ nm)
Fig. S19	Luminescence decay profiles of complexes <b>1</b> (left), <b>2</b> (middle) and <b>3</b> (right)
Table S1	Fitted parameters of the Cole-Cole plots for complex <b>1</b> at H <sub>dc</sub> = 0 G.
Table S2	Fitted parameters of the Cole-Cole plots for complex <b>2</b> at H <sub>dc</sub> = 0 G.
Table S3	Fitted parameters of the Cole-Cole plots for complex <b>3</b> at H <sub>dc</sub> = 0 G.



Scheme S1 Synthesis of complexes **1–3**.

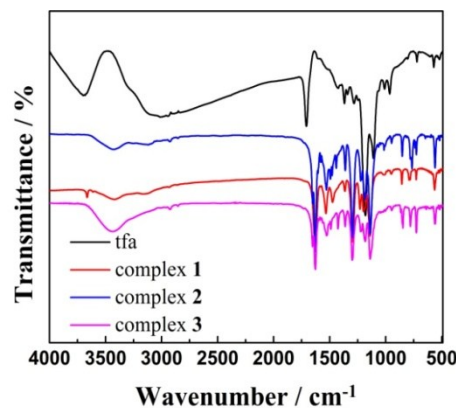


Fig. S1 IR spectra of tfa and complexes **1–3**.

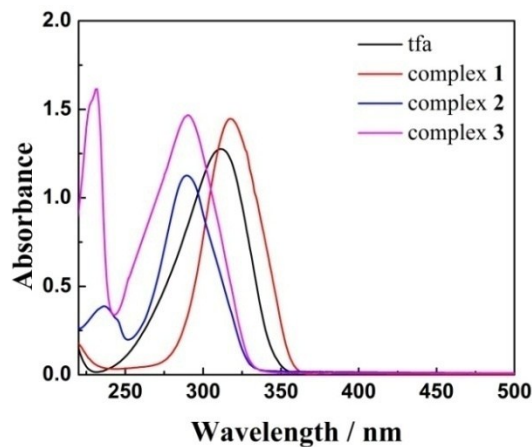


Fig. S2 UV-vis absorption spectra of tfa and complexes **1–3** in  $\text{CH}_3\text{OH}$  ( $10^{-5}$  mol/L).

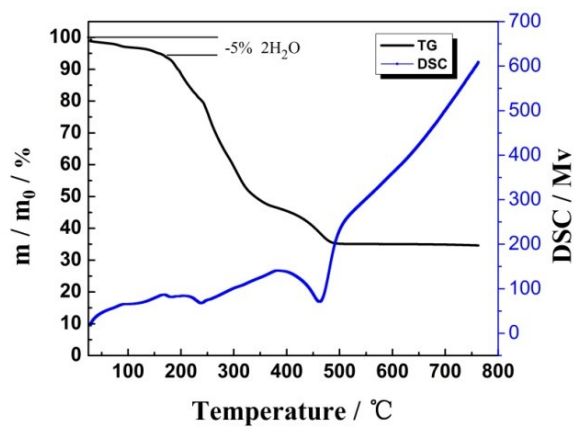


Fig. S3 TG–DSC curves of complex 1.

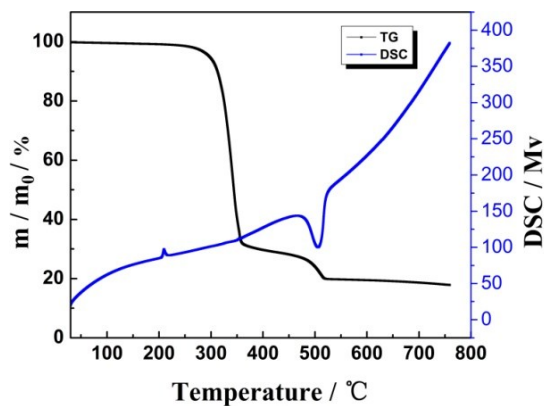


Fig. S4 TG–DSC curves of complex 2.

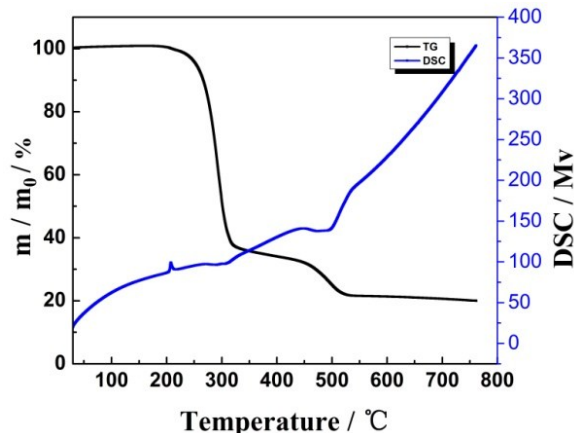


Fig. S5 TG–DSC curves of complex 3.

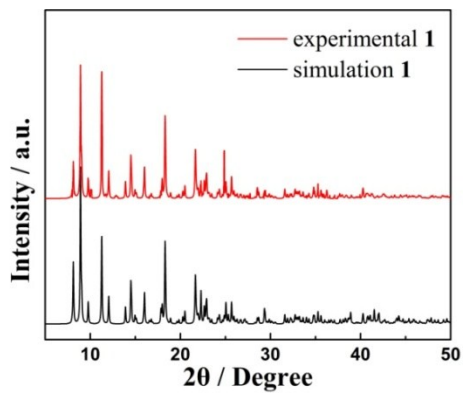


Fig. S6 The powder X–ray diffraction spectra of the simulated patterns and experimental for complex **1**.

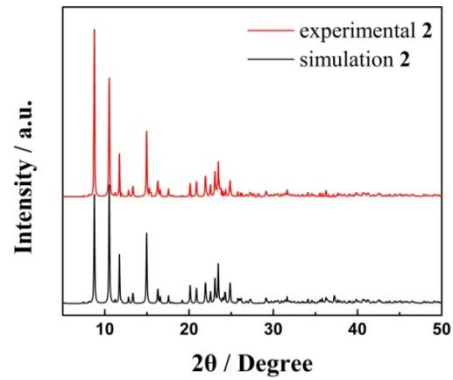


Fig. S7 The powder X–ray diffraction spectra of the simulated patterns and experimental for complex **2**.

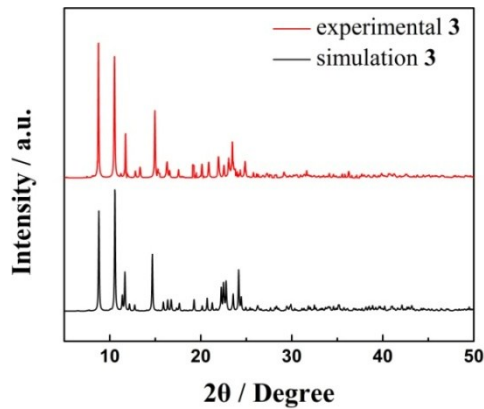


Fig. S8 The powder X–ray diffraction spectra of the simulated patterns and experimental for complex **3**.

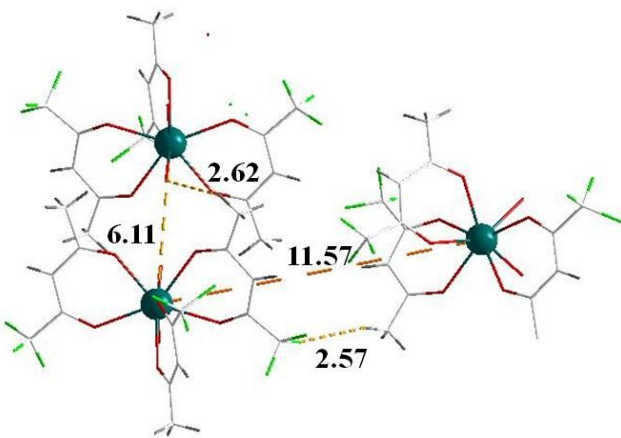


Fig. S9 The inter molecule hydrogen bonds interaction in complex 1.

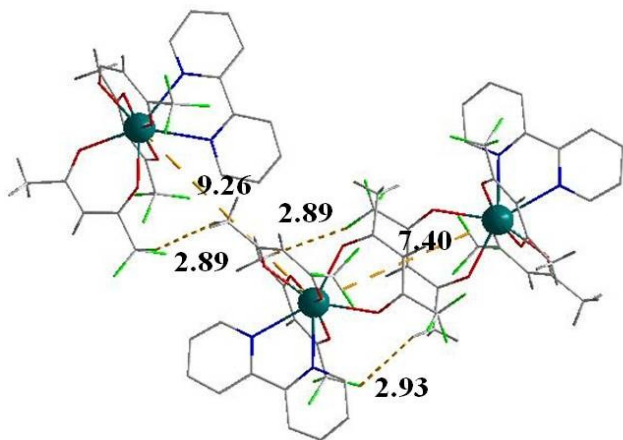


Fig. S10 The inter molecule hydrogen bonds interaction in complex 2.

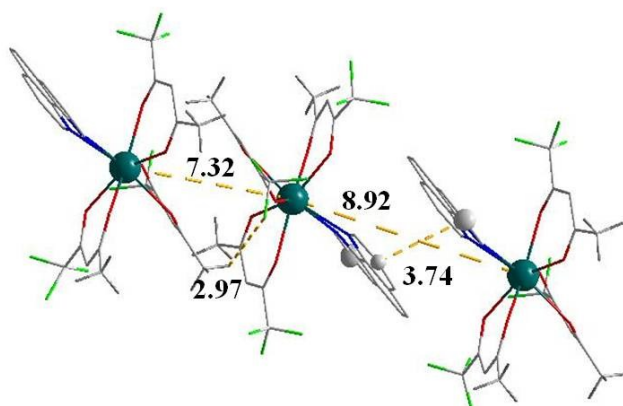


Fig. S11 The inter molecule  $\pi$ - $\pi$  stacking and hydrogen bonds interactions in complex 3

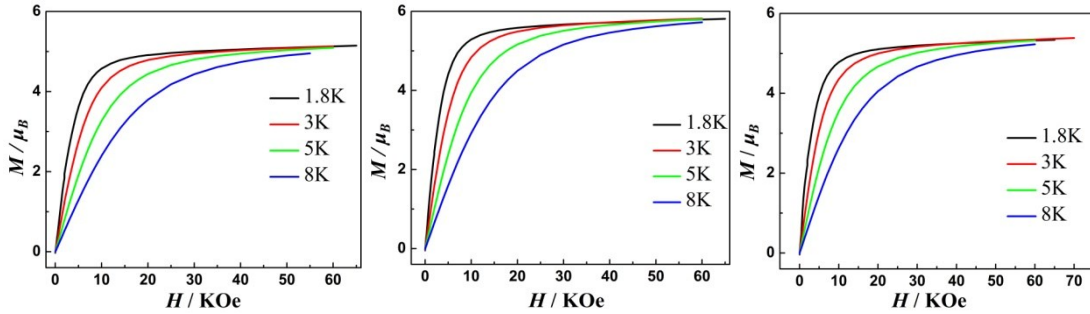


Fig. S12 M versus H / T plots at 1.8–8K for **1** (left), **2** (middle) and **3** (right).

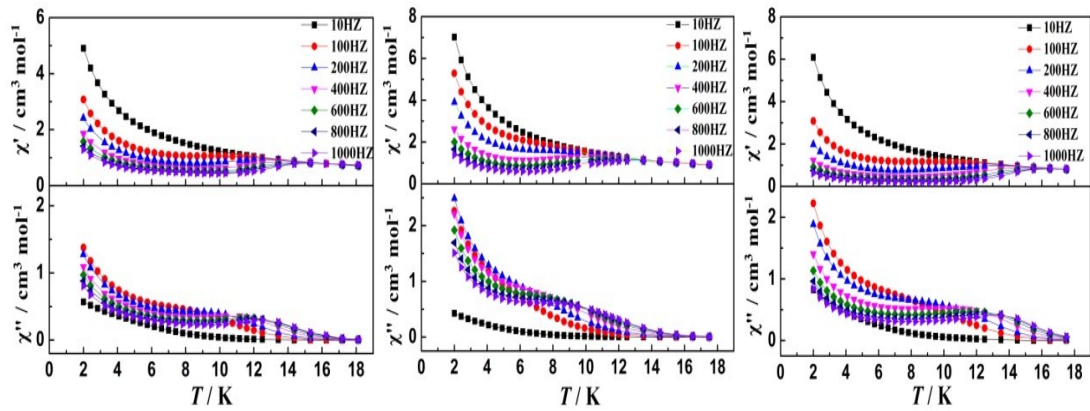


Fig. S13 Temperature dependence of the in-phase ( $\chi'$ ) and out-of-phase ( $\chi''$ ) ac susceptibility of complexes **1** (left), **2** (middle) and **3** (right), respectively, under zero dc field.

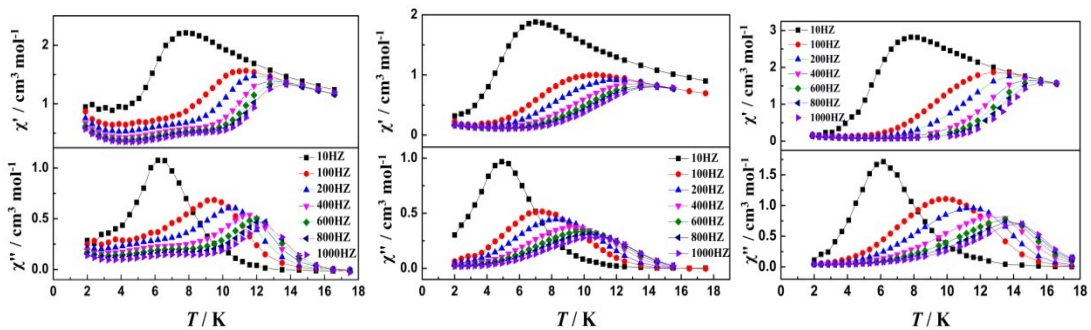


Fig. S14 Temperature dependence of the in-phase ( $\chi'$ ) and out-of-phase ( $\chi''$ ) acsusceptibility of complexes **1** (left), **2** (middle) and **3** (right) under 2000 Oe in the frequency range 10–1000 Hz in the temperature range of 2–18 K.

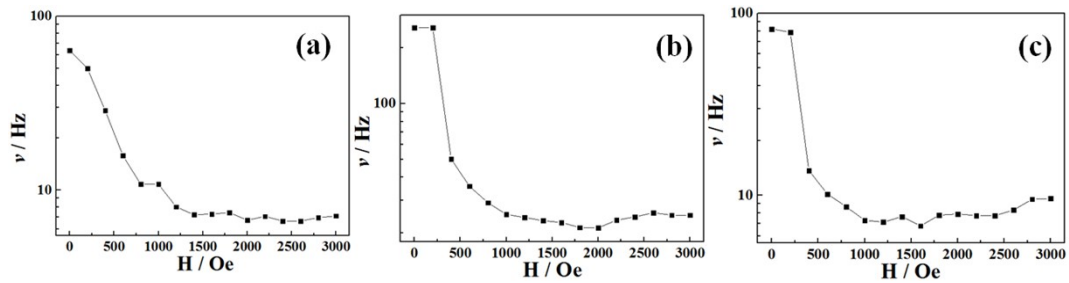


Fig. S15 Field dependence of the characteristic frequency as a function of the applied dc field for complexes **1** (a), **2** (b) and **3** (c) at 6 K.

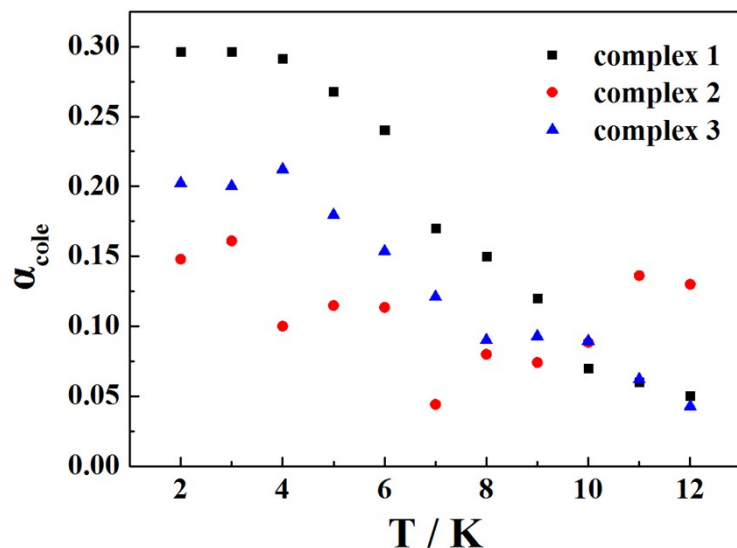


Fig. S16 Fitted broadness parameters  $\alpha_{\text{Cole}}$  as functions of temperature for complexes **1–3**.

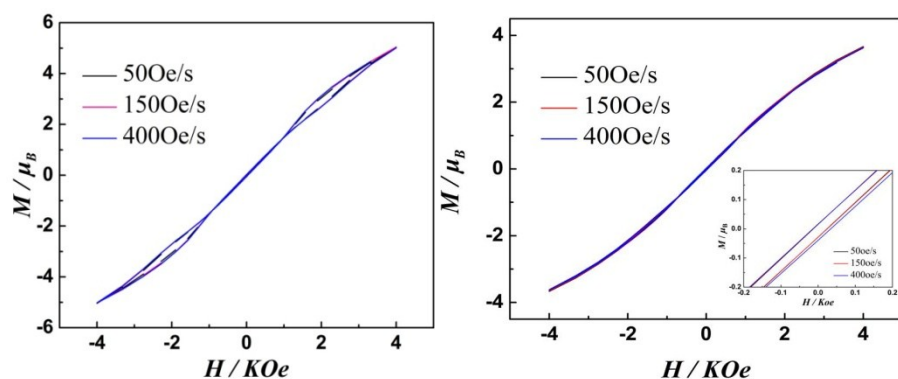


Fig. S17 Hysteresis loops for complexes **1** (left) and **2** (right) with different sweep rate at 1.8 K.

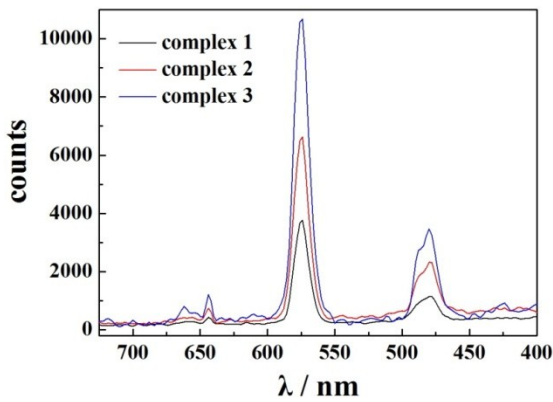


Fig. S18 Emission spectra of complexes **1–3** in the MeOH at 298 K ( $10^{-5}$  mol/L,  $\lambda_{\text{ex}} = 335$  nm).

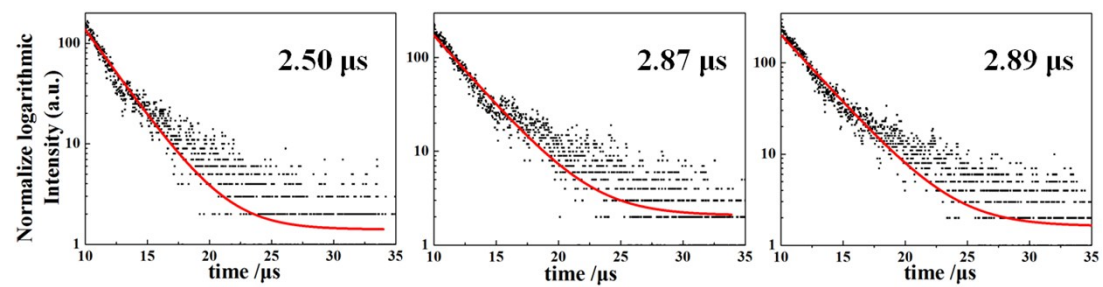


Fig. S19 Luminescence decay profiles of complexes **1** (left), **2** (middle) and **3** (right).

Table S1 Fitted parameters of the Cole-Cole plots for complex **1** at  $H_{\text{dc}} = 0$  G

T / K	$\chi_s$	$\chi_T$	$\tau$	$\alpha$
2.0	0.79821	7.90872	0.00155	0.29636
3.0	0.75419	5.74441	0.00197	0.29624
4.0	0.69267	4.52013	0.00219	0.29153
5.0	0.66000	3.71539	0.00221	0.26785
6.0	0.65997	3.18482	0.00218	0.24052
7.0	0.69400	2.75010	0.00188	0.17000
8.0	0.63711	2.44511	0.00148	0.15000
9.0	0.59284	2.18547	0.00108	0.12010
10.0	0.59010	1.95748	0.00068	0.07014
11.0	0.58636	1.80580	0.00048	0.06018
12.0	0.59104	1.65125	0.00024	0.05027

Table S2 Fitted parameters of the Cole-Cole plots for complex **2** at  $H_{dc}=0$  G

T / K	$\chi_s$	$\chi_T$	$\tau$	$\alpha$
2.0	2.52114	22.88511	0.00088	0.14803
3.0	1.46861	15.78451	0.00088	0.16102
4.0	1.99000	11.96630	0.00090	0.10010
5.0	1.54881	9.78260	0.00088	0.11484
6.0	1.56316	9.78074	0.00088	0.11350
7.0	2.09338	7.13911	0.00078	0.04412
8.0	2.49001	6.36585	0.00078	0.08001
9.0	2.84570	5.67926	0.00078	0.07403
10.0	3.16416	5.13107	0.00078	0.08847
11.0	3.34749	4.65563	0.00078	0.13618
12.0	3.46098	4.24383	0.00078	0.13000

 Table S3 Fitted parameters of the Cole-Cole plots for complex **3** at  $H_{dc}=0$  G

T / K	$\chi_s$	$\chi_T$	$\tau$	$\alpha$
2.0	0.24373	6.50042	0.00198	0.20235
3.0	0.19978	4.50003	0.00208	0.20011
4.0	0.15009	3.50000	0.00211	0.21229
5.0	0.11294	2.73849	0.00178	0.17964
6.0	0.12418	2.29602	0.00159	0.15367
7.0	0.18369	1.99358	0.00148	0.12102
8.0	0.19346	1.74521	0.00118	0.09009
9.0	0.09045	1.03579	0.00088	0.09285
10.0	0.09305	1.40321	0.00068	0.08947
11.0	0.12382	1.27521	0.00053	0.06212
12.0	0.16079	1.17750	0.00042	0.04274